Robert Citron was born in Silver Spring, MD and grew up in Overland Park, KS. He attended the University of Chicago, majoring in physics and math. As an undergraduate, he completed a SULI internship with the DOE and another internship with NASA. He plans to attend graduate school and study planetary science. His interests include science fiction, mountain biking, and Krav Maga.

Jeremy Kropf is a physicist in the Chemical Sciences and Engineering Division at Argonne National Laboratory. He received his Ph.D in Physics from the University of Notre Dame in 1997 for a study of interfacial structure in thin films and epitaxially-grown superlattices. His current research activities focus on applying X-ray absorption spectroscopy to energy-related challenges in the areas of catalysis, lithium-ion batteries, and the nuclear fuel cycle. He serves on the board of directors for the Materials Research Collaborative Access Team beamline at the Advanced Photon Source and the Beamline Advisory Team that is developing the plans for a new X-ray absorption spectroscopy facility at the proposed NSLS-II X-ray storage ring.

X-ray Absorption Spectroscopy of Yb^{3+}-Doped Optical Fibers

Robert Citron and A. Jeremy Kropf

ABSTRACT

Optical fibers doped with Ytterbium-3+ have become increasingly common in fiber lasers and amplifiers. Yb-doped fibers provide the capability to produce high power and short pulses at specific wavelengths, resulting in highly effective gain media. However, little is known about the local structure, distribution, and chemical coordination of Yb^{3+} in the fibers. This information is necessary to improve the manufacturing process and optical qualities of the fibers. Five fibers doped with Yb^{3+} were studied using Extended X-ray Absorption Fine Structure (EXAFS) spectroscopy and X-ray Absorption Near Edge Spectroscopy (XANES), in addition to Yb^{3+} mapping. The Yb^{3+} distribution in each fiber core was mapped with 2D and 1D intensity scans, which measured X-ray fluorescence over the scan areas. Two of the five fibers examined showed highly irregular Yb^{3+} distributions in the core center. In four of the five fibers Yb^{3+} was detected outside of the given fiber core dimensions, suggesting possible Yb^{3+} diffusion from the core, manufacturing error, or both. X-ray absorption spectroscopy (XAS) analysis has so far proven inconclusive, but did show that the fibers had differing EXAFS spectra. The Yb^{3+} distribution mapping proved highly useful, but additional modeling and examination of fiber preforms must be conducted to improve XAS analysis, which has been shown to have great potential for the study of similar optical fibers.

INTRODUCTION

Rare earth (RE) doped optical fibers have rapidly been gaining attention for use in fiber lasers and amplifiers. Yb^{3+}-doped fibers are particularly effective because their higher doping levels result in higher output power and efficiency [1, 2]. But, despite their advantages, Yb-doped fibers are still prone to problems. Clustering is a problem when higher concentrations of REs are present [3–5] and can lead to concentration quenching [6] and reduction in radiative transitions [7]. Higher Yb^{3+} concentration can also reduce gain by means of cooperative upconversion [1].

Many of the problems associated with Yb-doped fibers result from the manufacturing process, which determines the local structure of Yb^{3+} in the fibers. Determining and understanding the local structure of Yb^{3+} in the fibers is critical to finding ways to improve fiber manufacturing and increasing the optical qualities of the fibers.

The aim of this experiment was to examine the distribution and local structure of Yb^{3+} in fibers using Extended X-ray Absorption Fine Structure spectroscopy (EXAFS), X-ray Absorption Near Edge Spectroscopy (XANES), and Yb^{3+} concentration mapping. The

distribution of Yb^{3+} should display radial symmetry; any asymmetrical behavior, diffusion into the cladding, or a concentration depression towards the center of the core could have detrimental effects on the efficiency of the fibers [8].

Prior studies of RE doped fibers examined the fiber glass preforms or the fibers themselves. Some used instruments such as the ion microprobe [9] or Raman confocal microscope [8]. Previous studies also included EXAFS [3, 6, 10–12] and XANES [4, 13, 14], but most investigated other REs such as erbium. Some X-ray Absorption Spectroscopy (XAS) studies have investigated the Yb^{3+} local structure in glass [5], but, to the best of our knowledge, this is the first EXAFS and XANES measurement of Yb^{3+} in fibers.

MATERIALS AND METHODS

X-ray Fluorescence Mapping

X-ray fluorescence mapping is a useful tool for finding the distribution of elements, such as Yb, in materials. Incident x-rays are set to an energy equal to, or slightly above, the absorption edge of the targeted element. At this energy, there will be a sharp rise in

absorption. Excited electrons will move to higher energy levels and quickly decay, releasing photoelectrons and fluorescence photons [15]. An x-ray fluorescence detector will measure higher or lower count rates depending on the concentration of the targeted element at each point in the mapped region. By focusing the beam to a small area (<9 μm^2) and moving the beam in a grid pattern or a simple line scan, the x-ray fluorescence at each point can be measured. This will display the distribution and concentration of the targeted element in the sample. In this experiment, line and grid scans were taken of Yb^{3+} X-ray fluorescence from the core of the fibers. The germanium distribution was also mapped in one fiber.

XAS

X-ray Absorption Spectroscopy (XAS) is well-suited for determining the local structure and chemical coordination of Yb^{3+} ions in optical fibers. XAS can be divided into two main categories: Extended X-ray Absorption Fine-Structure (EXAFS) and X-ray Absorption Near Edge Spectroscopy (XANES). EXAFS is suitable for determining the distance, coordination number, and the neighboring species of the Yb^{3+} ion. XANES is useful for detecting the coordination chemistry, bond structure, molecular orbitals, and multiple scattering from the Yb^{3+} ions.

The Advanced Photon Source synchrotron facility at Argonne National Laboratory produces a steady X-ray source well suited for XAS experiments. The experiment was conducted at Sector 10-ID, MR-CAT.

Sample Preparation

Five optical fibers provided by Southampton Photonics were examined. The fibers had varying core diameters and Yb^{3+} concentrations (Table 1). Before being examined with XAS, the fibers were cut into thin cross-sections suitable for X-ray measurements.

Fiber Number	Fiber ID	Core Diameter (µm)	Cladding Diameter (µm)	Yb^{3+} Concentration (ppm)
1	T0084 L30058	43	670	4500
2	P004 F01	12	125	5500
3	T0075 P120	30	400	13000
4*	F125 FI24	30	375	6500
5**	T0072 ROD2	25	290	20000
*Contains a central dip.				
**Inter cladding contains GeO_2				

Table 1

The x-rays will penetrate through <100 µm of the fiber samples, but, in order to obtain improved results, the fibers had to be cut to a thickness of significantly less than 100 µm. The ideal thickness would be less than 20 µm. The faces of the fiber were polished to reduce surface disturbance and further improve the results.

Each sample was first embedded in an epoxy made from Buehler Epoxicure/Epoxide resin and hardener. This created a cylindrical stub with the fiber along the vertical axis (Figure 1a). The top of the stub was then cut with a low speed diamond saw to create a flat surface for polishing. The top face was then polished using 320 and 600 grit paper and ending with a 15 µm diamond polish which leaves grooves <2 µm deep.
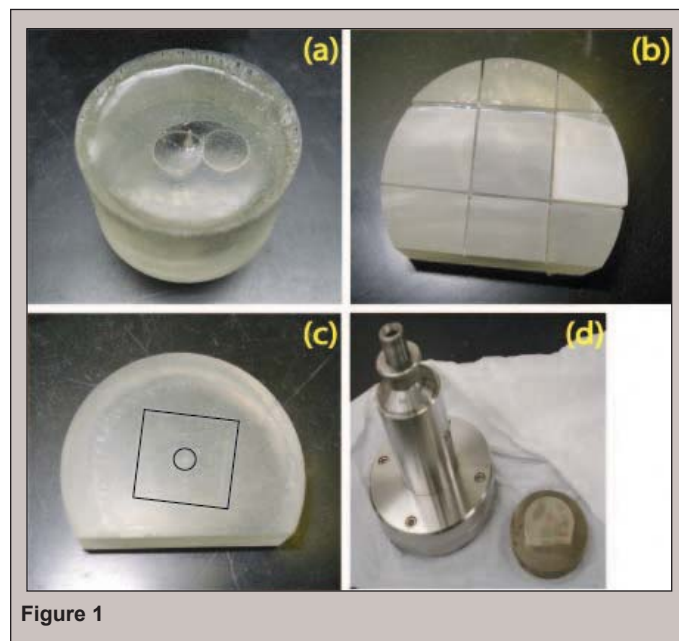

Figure 1

After polishing the top face, a thin square about 1 cm^2 and less than 1 mm in thickness was cut from the polished face of the stub (Figure 1b). The thickness of the square was precisely measured before it was re-embedded in epoxy. It was re-embedded so that its unpolished side was facing down, at the very bottom of the sample holder (Figure 1c). After the epoxy hardened, the sample was again cut so that it could fit in a polishing mount to be precisely polished/re-polished (Figure 1d). The goal was to orient the precisely measured square section at the bottom of the new epoxy stub so that it could be precisely ground. For example, if the square section had an average thickness of .8 mm, the goal would be to remove .700–.780 mm of material so that a very thin fiber section could be examined with XAS.

The sample was fixed to a polishing fixture that could be used to remove a specific amount of material. A small amount of epoxy seeped under the sample during preparation, so first the sample was polished until the epoxy that seeped under the square section was removed (i.e. when the bubbles that formed under the square section disappeared). This position was noted as the zero position and the thickness of the stub was measured with a micrometer. Since the exact thickness of the square section containing the fiber was measured before re-embedding, it was possible to measure the thickness of the embedded fiber sample during polishing by measuring the amount of material removed using a micrometer. In this manner the sample could be polished to a thickness of 50–100 µm (20 µm proved too risky) using 400, 800, and 1200 grit paper with a final polish using 15 µm diamond. It was noted that coarser paper caused too much damage to the fiber.

Fibers 1–3 were prepared in this manner. Fiber 4 ripped out during polishing when it became too thin and there was insufficient time to prepare samples 5–7 in this manner. The initial epoxy-embedded stubs of fibers 4 and 5 were cut and polished so they could be examined using XAFS, even though they were not thin sections.

XAS and X-ray mapping setup

The fibers were examined using x-ray fluorescence. They were placed so that the incident X-rays were parallel to the fiber axis. A germanium detector (Canberra Industries, Ultra-LEGe 19 element array) was used in the configuration seen in Figure 2. The beam energy was set to 11.500 KeV to excite both Yb^{3+} and Ge atoms as well as to allow for Yb L3 absorption edge measurements. The X-ray beam was focused to 3 μm^2 using total external reflection mirrors in the Kirkpatrick-Baez geometry, which allowed for high resolution intensity scans of the fiber core.

Figure 2
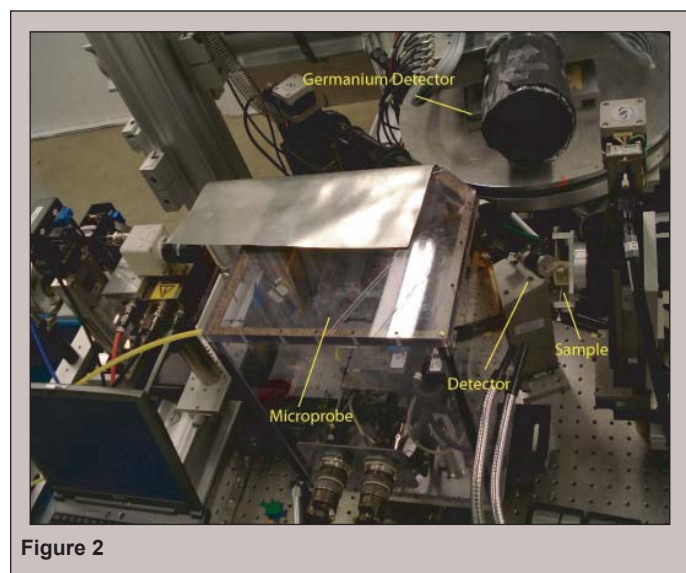
After locating each fiber, a 2D intensity grid scan was taken of the core to measure the ytterbium concentration in the core. Line scans were then taken on the orthogonal axes through the center of the core. After noting the distribution from the 2D map, 1–4 locations were selected for EXAFS and XANES scans. Due to time constraints, some samples were scanned only once, while others were given multiple scans at different locations. The locations were chosen so they best reflected the entire fiber core. Scans were taken at sites of high and low Yb^{3+} concentration for comparison.

Results and Discussion

Ytterbium Distribution

Figure 3 displays contour plots from the 2D intensity scans of each fiber. The scans show that the Yb^{3+} distribution in the cores of the fibers is not uniform. The Yb^{3+} distribution concentrates at a peak and then spreads outward. Fibers 2 and 5 show fairly

symmetrical cores, with higher intensity peaks towards the center of the core. Fiber 4 also contains an almost symmetrical peak at the center of the core. Fibers 1 and 3, however, display crescent shaped Yb^{3+} distributions. After scanning Fiber 1, the fiber was rotated 180 degrees and rescanned to ensure that the crescent distribution was not a result of the experimental setup and geometry. The resulting scan displayed the same image as before, but rotated 180 degrees, confirming that the lopsided nature of the image is due to the Yb^{3+} distribution in the core. Fibers 1 and 3 both display similar crescent peaks that appear to be a result of manufacturing error. During manufacturing, fibers are drawn out at high temperature to form the thin fibers of the final product. This process is prone to error because it is difficult to maintain a circular cross-section, sometimes the cladding of the fiber will collapse into the fiber core. Such a collapse seems the most likely explanation for the irregular distributions observed in fibers 1 and 3.

The germanium distribution in the inner cladding of Fiber 5 is shown in Figure 3f. There is a narrow space between the core and the inner cladding where the Yb^{3+} and Ge concentrations both dip. This is emphasized in the overlay of the Yb^{3+} and Ge grid maps (Figure 5). The germanium distribution is slightly lopsided, but this does not seem to have affected the symmetrical Yb^{3+} distribution in the core.

Linescans taken through the center of each core along the X and Y axes better display the shape of the Yb^{3+} peaks (Figure 4). Yb^{3+} distributions with flat-topped peaks would be preferred and show the most uniform distribution of Yb^{3+} in the fiber core. Most peaks display a rounded point(s) at the top. Fiber 5 displays the flattest peak, which is also observed in the broad red area in the Fiber 5 contour plot. The linescans were used to accurately measure the width of the Yb^{3+} distribution in the fiber cores. Measurements were made at the turning point where the peak begins to meld into the background. Full-width half-maximum (FWHM) measurements were also made. Both were compared to the widths of the cores provided by the manufacturer (Table 2). With the exception of Fiber 4, the Yb^{3+} distribution peaks were wider than the fiber core diameters provided by the manufacturer. This implies that either the fiber cores were wider than the given dimensions or the Yb^{3+} ions diffused outside the fiber cores. The irregular pattern of the Yb^{3+} concentration towards the edge of the Yb^{3+} peak seen in the contour plots (Figure 3) suggest that the Yb^{3+} diffused from the core. The cores would not be expected to stretch into the irregular shapes seen in Figures 3a–e due to manufacturing error. However,

Fiber number	Given core width (μm)	Avg. Yb^{3+} width (μm)	Fwhm (μm)	Difference* (μm)	Yb^{3+} concentration (ppm)
1	43	57.0 ± 4	38.2 ± 0.9	14	4500
2	12	29.0 ± 3	12.9 ± 0.3	17	5500
3	30	76.5 ± 4	52.7 ± 0.9	46.5	13000
4	30	25.5 ± 5	15.1 ± 0.3	-4.5	6500
5	25	34.5 ± 4	25.1 ± 0.2	9.5	20000
*Difference between the experimental Yb^{3+} peak width and the fiber core diameter (from Table 1).					

Table 2

inaccuracies in the manufacturing process mean that the cores could differ from the provided dimensions. The distributions could result from manufacturing error, diffusion (the difference between the experimental and given core widths), or both. Further studies should

include refractive index measurements to see the exact dimensions of the core and to see how the core mixes with the cladding.

No real correlation between Yb^{3+} concentration and possible diffusion was found. The full-width half-maxima also display no
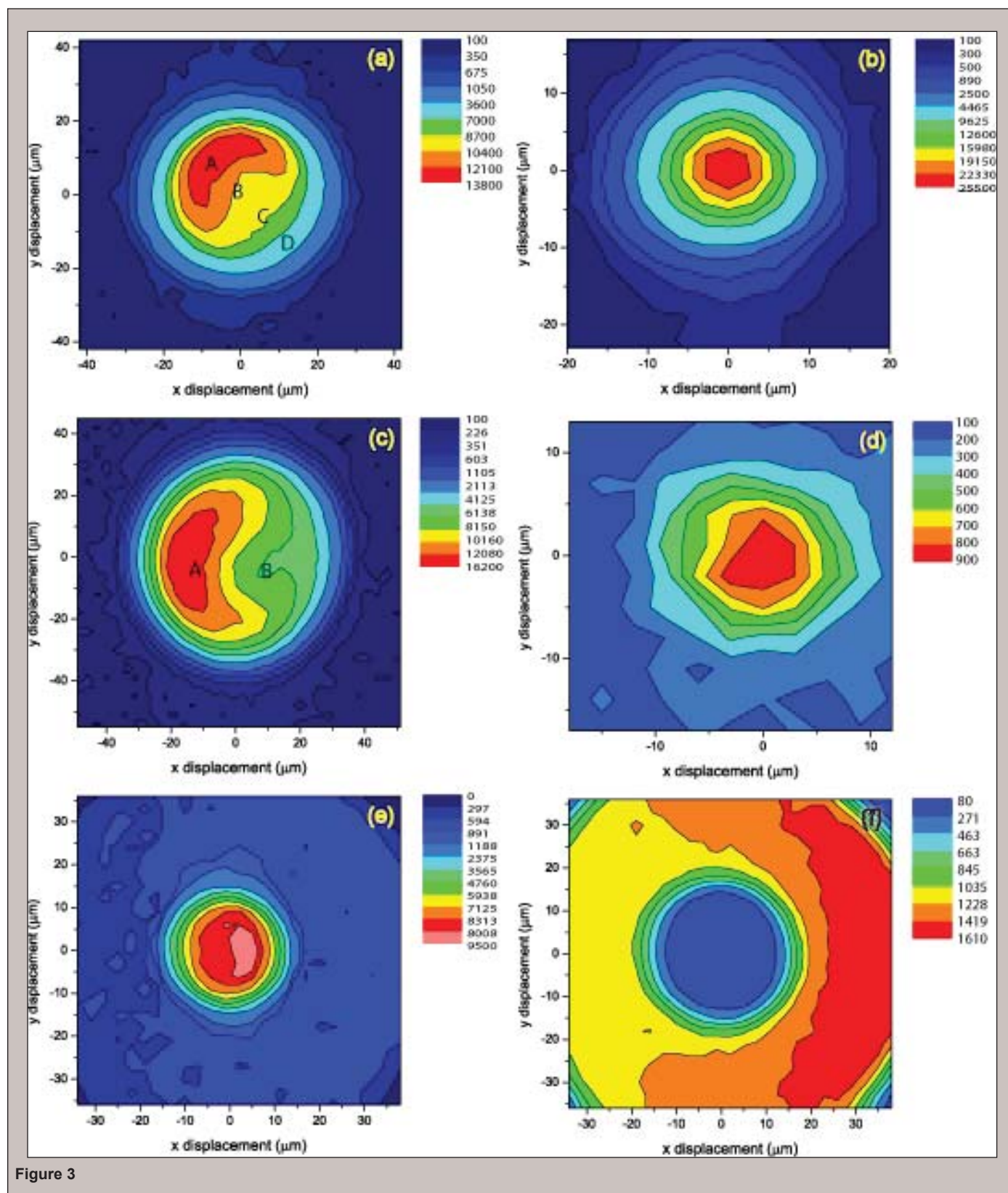
Figure 3

clear relation to the Yb^{3+} concentrations or given core widths. Fibers 1–3 display an almost linear relation between Yb^{3+} concentration and possible diffusion, but Fibers 4 and 5 display no such correlation. This may be because of their unique properties (central dip and cladding Ge content, respectively).

EXAFS and XANES Interpretation

The EXAFS data was analyzed using standard methods with the IFEFFIT program suite. ATHENA was used for background subtraction and summing multiple data sets. ARTEMIS was used
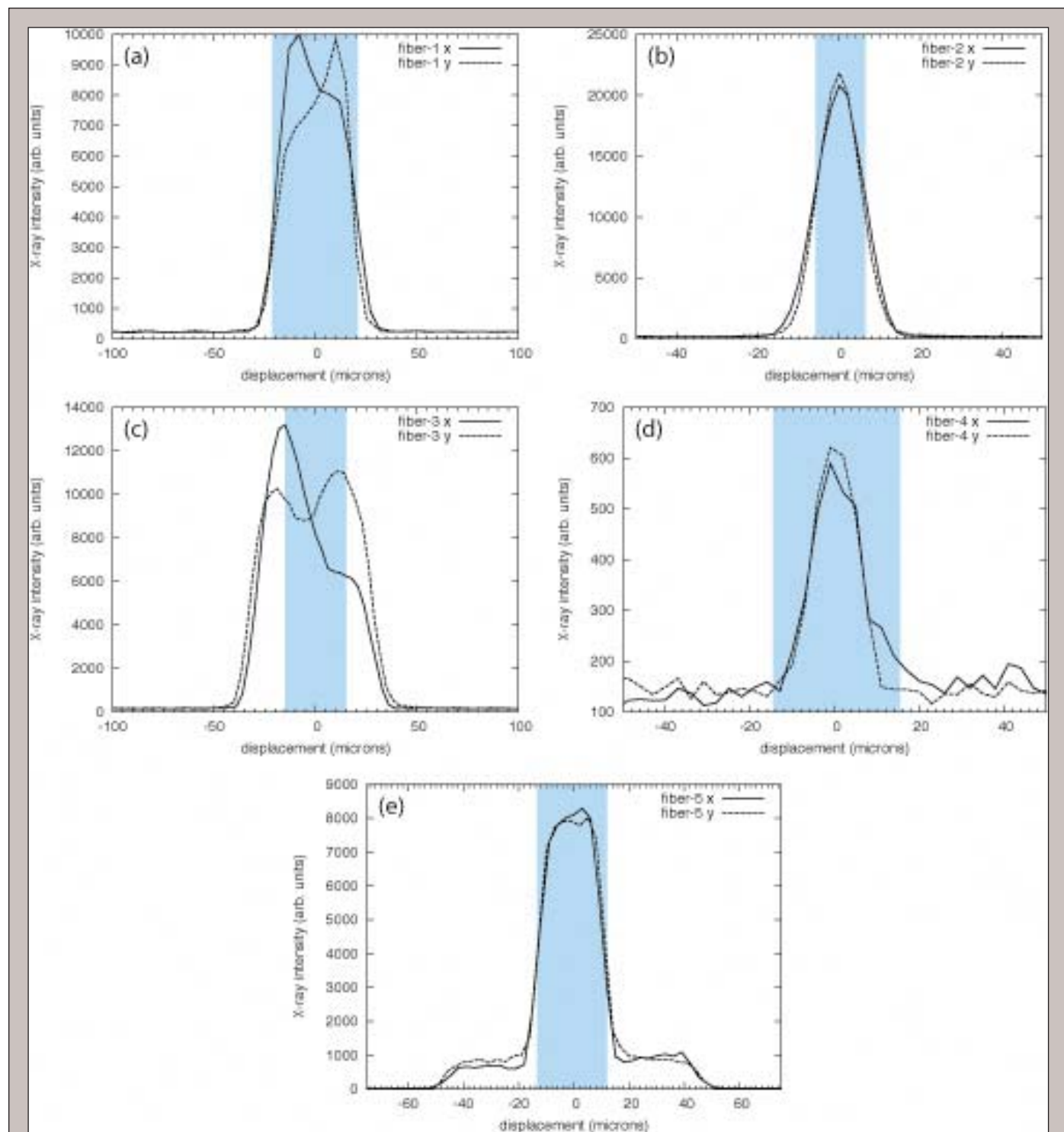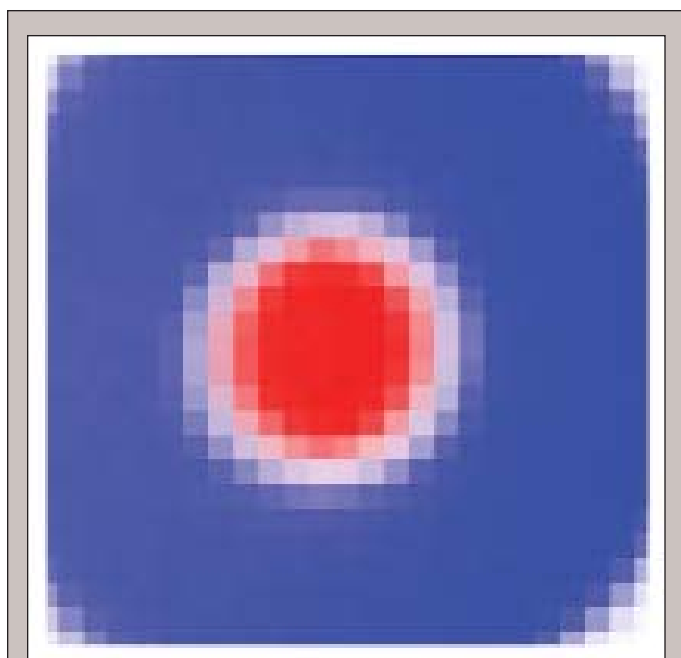

Figure 4

U.S. Department of Energy Journal of Undergraduate Research

43

http://www.scied.science.doe.gov

Figure 5

to fit the data using theoretical models made with FEFF. The basic EXAFS equation is:

$$\chi(k) = \sum_j \frac{N_j e^{-2k^2 \sigma^2_j} e^{-2R_j/\lambda(k)} f_j(k)}{kR_j^2} \sin[2kR_j + \delta_j(k)]$$

where N_j is the number of neighboring atoms at a distance of R_j with a disorder in the neighboring distance of σ_j^2, and $f_j(k)$ and $\delta_j(k)$ represent neighboring atom and excited atom scattering properties [15].

Using plots of $\chi(k)$ and $\chi(R)$, the different EXAFS spectra between the different fibers (Figure 6) and between different locations in the same fiber (Figure 7) were compared. The data from Fibers 2 and 4 were too noisy, but fibers 1, 3, and 5 were comparable. Each of the fibers displays a modestly different EXAFS spectrum. The Fiber 5 spectrum appears to be a mix of the fiber 1 and 3 spectra, having an average amplitude between that of fiber 1 and 3.

The different locations in the cores of Fiber 1 and 3 (Figure 7) display very similar plots in k-space, though position C contains less noise and has a smaller amplitude. In R-space the spectra have more drastic differences. This could be caused by differences in Yb^{3+} concentrations within the fiber core. In Fiber 1, from position A to C the Yb^{3+} concentration decreased as seen in Figure 3. In Figure
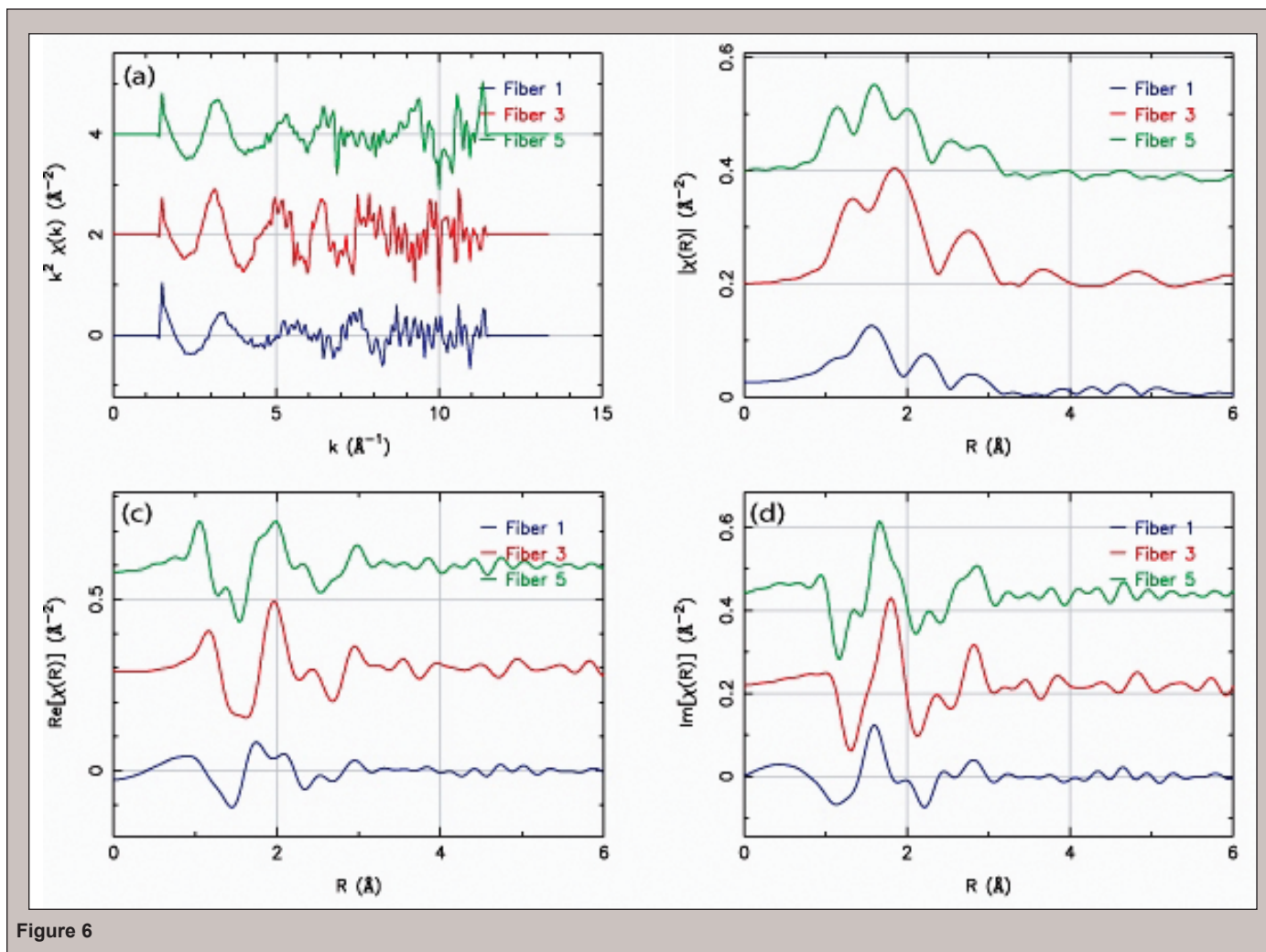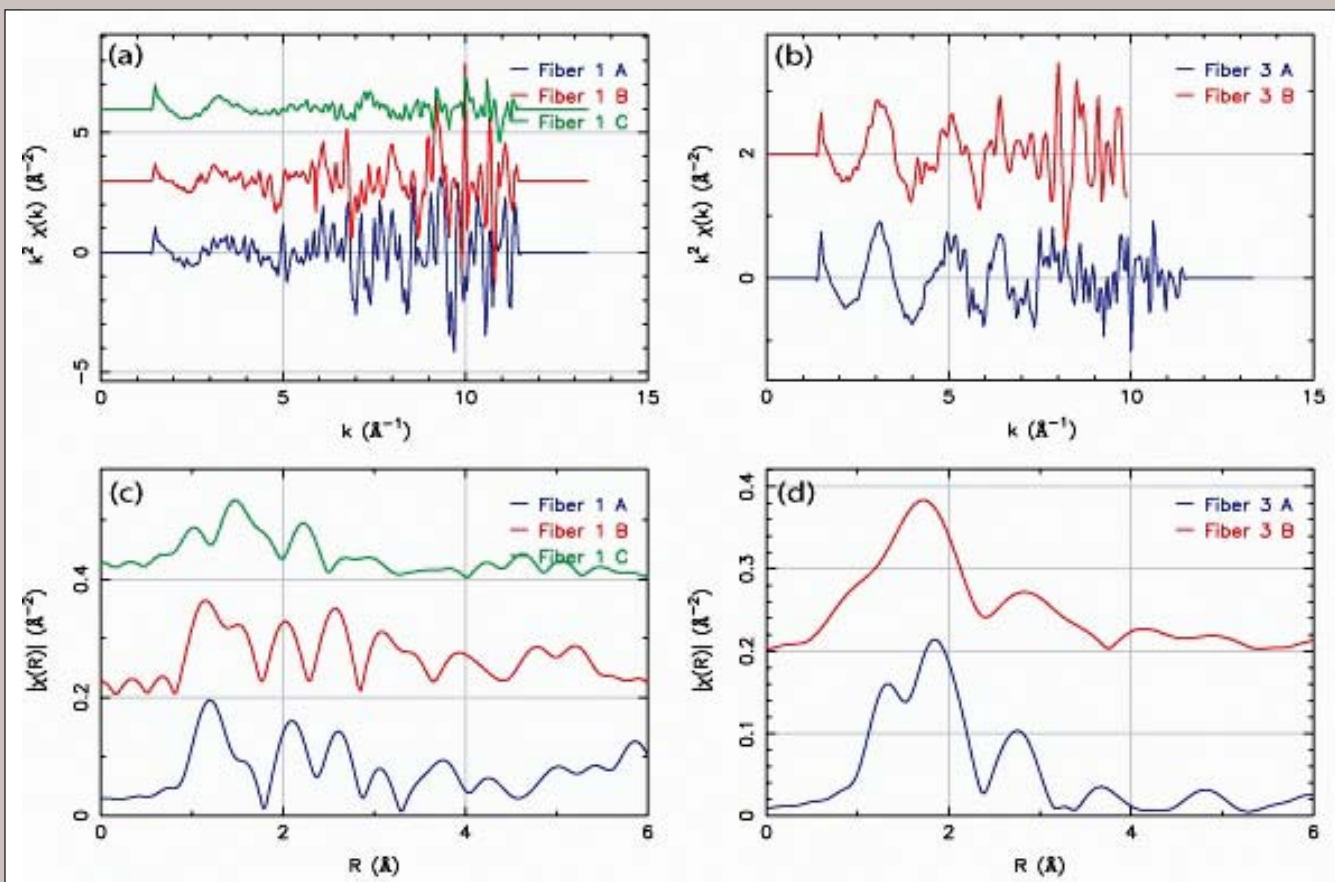

Figure 6

Figure 7

7c, from positions A to C, it appears that the larger first peak at 1.1 Å diminishes as the peak at 1.7 Å takes over. A similar effect is seen in Fiber 3 (Figure 7d).

Unfortunately, no conclusive fit was made to the measured EXAFS data. The data from Fiber 4 and Fiber 2 were too noisy. Fibers 1 and 5 had unexpectedly low initial amplitudes and the fits did not produce realistic results. This resulted from interference in spectra from different photoelectron scattering paths. If this persists, then the problem may not be solvable using EXAFS. However, Fiber 3 had a better initial amplitude and less peak interference. It produced unrealistic but improved results. Work is still being conducted to refine the fitting process and to produce interpretable results.

Figure 8 displays the XANES spectra for Fibers 1, 3 and 5, and for separate locations within the core of Fiber 1 and 3. Each fiber displays a unique spectrum, which is important information
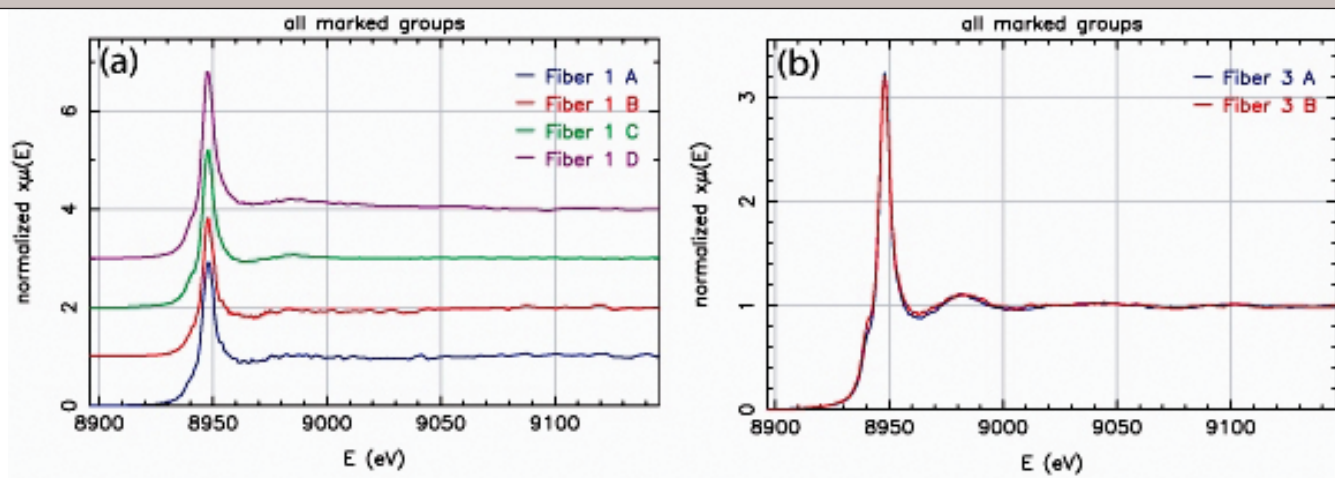

Figure 8

itself, showing that the differences in Yb^{3+} concentration and fiber production do produce different local structures. In Fiber 1, a bump in the upwards slope at 8940 eV appears at locations A and B, which are at higher Yb^{3+} concentrations than locations C and D. In Fiber 3, this feature appears to become larger from position B to A, or from lower to higher Yb^{3+} concentration. The bump may possibly be a characteristic of higher Yb^{3+} concentrated regions. As for the specific interpretation of the XANES spectra, further analysis cannot be completed until XANES measurements are made of the fiber optic preforms so that comparisons between the experimental data and known configurations can be made.

Conclusion

Five fibers were analyzed using X-ray absorption spectroscopy. The fibers were made into thin sections and analyzed with 1D and 2D X-ray fluorescence mapping scans in addition to EXAFS and XANES scans. There was no significant difference in the spatial resolution for the Yb maps for fibers that were prepared 50–100 μm thick and those that were much larger. Future studies should find methods to obtain samples less than 20 μm thick. The 2D intensity scans of the fiber cores were extremely useful, revealing information on the fiber cores. The cores were found to be diffusing Yb^{3+} into the cladding, larger than manufacturer dimensions, or both. The extent of diffusion can be resolved through a comparison of the linescans with refractive index as done in a previous study using a Raman confocal microscope [8]. Two fibers also displayed signs of collapse during manufacturing. The scan of Fiber 5 also displayed a depression between the Yb^{3+} and the GeO_2 in the core and cladding. The grid scans and line scans proved a useful tool to search for fiber collapse and diffusion, though future studies should include refractive index measurements.

Each fiber displayed a unique EXAFS and XANES spectrum, suggesting there is much to be learned from studying the fiber cores further. There were also slight variations in the XANES and EXAFS scans within the individual fiber cores. These variations could be caused by drops in the Yb^{3+} concentration. EXAFS fitting was unsuccessful due to the low amplitude of the spectra and interference between peaks. In order to produce a comprehensive XANES analysis, fiber preforms must be obtained to compare to the fiber core XANES data. Different samples may produce more easily fit results for EXAFS analysis. The distribution maps were highly successful, and the described enhancements to XANES and EXAFS analysis could make XAS a very useful tool for optical fiber analysis.

Acknowledgments

References

[1] R. Paschotta, J. Nilsson, A. C. Tropper, and D. C. Hanna, "Ytterbium-doped fiber amplifiers," *IEEE Journal of Quantum Electronics*, vol. 33, no. 7, pp. 1049–1056, Jul. 1997.

[2] H. M. Pask, R. J. Carman, D. C. Hanna, A. C. Tropper, C. J. Mackechnie, P. R. Barber, and J. M. Dawes, "Ytterbium-doped silica fiber lasers — versatile sources for the 1-1.2 MU-M region," *IEEE Journal of Selected Topics in Quantum Electronics*, vol. 1, no. 1, pp. 2–13, Apr. 1995.

[3] J. C. Du and A. N. Cormack, "The structure of erbium doped sodium silicate glasses," *Journal of Non-Crystalline Solids*, vol. 251, no. 27-29, pp. 2263–2276, Aug. 2005.

[4] R. M. Almeida, H. C. Vasconcelos, M. C. Goncalves, and L. F. Santos, "XPS and NEXAFS studies of rare-earth doped amorphous sol-gel films," *Journal of Non-Crystalline Solids*, vol. 234, pp. 65–71, Jul. 1998.

[5] J. A. Sampaio and S. Gama, "EXAFS investigation of local structure of Er^{3+} and Yb^{3+} in low-silica calcium aluminate glasses," *Physical Review B*, vol. 69, no. 10, p. 104203, Mar. 2004.

[6] P. M. Peters and S. N. HoudeWalter, "X-ray absorption fine structure determination of the local environment of Er^{3+} in glass," *Applied Physics Letters*, vol. 70, no. 5, pp. 541–543, Feb. 1997.

[7] B. J. Ainslie, "A review of the fabrication and properties of erbium-doped fibers for optical amplifiers," *Journal of Lightwave Technology*, vol. 9, no. 2, pp. 220–227, Feb. 1991.

[8] F. Sidiroglou, S. T. Huntington, and A. Roberts, "Micro-characterisation of erbium-doped fibers using a raman confocal microscope," *Optics Express*, vol. 13, no. 14, pp. 5506–5512, Jul. 2005.

[9] F. Sidiroglou, S. T. Huntington, A. Roberst, R. Stern, and I. R. Fletcher, "Simultaneous multidopant investigation of rare-earth-doped optical fibers by an ion microprobe," *Optics Letters*, vol. 31, no. 22, pp. 3258–3260, Nov. 2006.

[10] S. Gurman, R. J. Newport, M. Oversluizen, and E. J. Tarbox, "An extended x-ray absorption fine-structure study of the rare-earth sites in a neodymium doped glass," *Physics and Chemistry of Glasses*, vol. 33, no. 1, pp. 30–32, Feb. 1992.

[11] D. T. Bowron, R. J. Newport, J. S. Rigden, E. J. Tarbos, and M. Oversluizen, "An X-ray absorption study of doped silicate glass, fibre optic preforms," *Journal of Materials Science*, vol. 31, no. 2, pp. 485–490, Jan. 1996.

[12] M. A. Marcus and A. Polman, "Local-structure around Er in silica and sodium-silicate glasses," *Journal of Non-Crystalline Solids*, vol. 136, no. 3, pp. 260–265, Dec. 1991.

[13] T. Haruna, J. Iihara, K. Yamaguchi, Y. Saito, S. Ishikawa, M. Onishi, and T. Murata, "Local structure analyses around Er^{3+}in Er-doped fiber with Al co-doping," *Optics Express*, vol. 14, no. 23, pp. 11 036–11 042, Nov. 2006.

[14] M. R. Antonio, L. Soderholm, and A. J. G. Ellison, "Local environments of erbium and lutetium in sodium silicate glasses," *Journal of Alloys and Compounds*, vol. 250, no. 1-2, pp. 536–540, Mar. 1997.

[15] M. Newville. (2004, Jul.) Fundamentals of XAFS. Consortium for Advanced Radiation Sources. [Online]. Available: http://xafs.org/Tutorials